Drug Design, Development and Therapy

Dovepress
open access to scientific and medical research

Open Access Full Text Article

ORIGINAL RESEARCH

Yishen Qingli Heluo Granule in the Treatment of Chronic Kidney Disease: Network Pharmacology Analysis and Experimental Validation

Xian Sun[1], Yiting Huang[1], Sha Zhu[1], Jin Yan[2], Ke Gan[3], Zijing Xu[4], Shuaishuai Wang[4], Xiaoyu Kang[4], Junfeng Zhang[4], Wei Sun[2]

[1]The First Clinical Medical College, Nanjing University of Chinese Medicine, Nanjing, 210023, People's Republic of China; [2]Department of Nephrology, Jiangsu Province Hospital of Chinese Medicine, Affiliated Hospital of Nanjing University of Chinese Medicine, Nanjing, 210029, People's Republic of China; [3]Department of Rheumatology, Jiangsu Province Hospital of Chinese Medicine, Affiliated Hospital of Nanjing University of Chinese Medicine, Nanjing, 210029, People's Republic of China; [4]School of Medicine & Holistic Integrative Medicine, Nanjing University of Chinese Medicine, Nanjing, 210023, People's Republic of China

Correspondence: Wei Sun, Department of Nephrology, Jiangsu Province Hospital of Chinese Medicine, Affiliated Hospital of Nanjing University of Chinese Medicine, Nanjing, 210029, People's Republic of China, Tel +86-13505199810, Email yfy0074@njucm.edu.cn; Junfeng Zhang, School of Medicine & Holistic Integrative Medicine, Nanjing University of Chinese Medicine, Nanjing, 210023, People's Republic of China, Tel +86-13805186836, Email Zhangjunfeng419@njucm.edu.cn

Video abstract

Point your SmartPhone at the code above. If you have a QR code reader the video abstract will appear. Or use: https://youtu.be/02pumepfbPI

Background: Chronic kidney disease (CKD) is considered a global public health problem with high morbidity and mortality. Yishen Qingli Heluo granule (YQHG) is representative traditional Chinese medicine (TCM) remedy for clinical treatment of CKD. This study aims to explore the mechanism of YQHG on CKD through network pharmacology and experimental validation.

Methods: Traditional Chinese Medicine Systems Pharmacology (TCMSP) database and wide-scale literature mining were applied to screen active compounds of YQHG. Multiple bioinformatic tools and online databases were applied by us to obtain relevant targets of YQHG and CKD. The intersection targets between YQHG and CKD were considered as candidate targets. The compound-target, herb-candidate target and protein–protein interaction networks were constructed and visualized for topological analyses. GO and KEGG enrichment analyses were conducted to determine the biological processes and signaling pathways. Molecular docking was used to verify the reliability of network pharmacology. Finally, pharmacological evaluation was performed to explore the mechanism of YQHG against CKD on a 5/6 nephrectomy model.

Results: Seventy-nine candidate targets, ten core biological processes and one key signaling pathway (p53) were screened. PTGS2 was identified as a key target based on H-CT network. The molecular docking showed that Quercetin, Kaempferol, Luteolin were three key compounds with the best binding activity. In addition, IL6 and Quercetin could form a stable complex with high binding affinity (−7.29 kcal/mol). In vivo experiment revealed that YQHG improved kidney function and fibrosis in 5/6 nephrectomized rats. Moreover, the decreased expression of PTGS2, IL6, and the increased expression of p53 were observed in kidney tissue. Notably, the gut microbiota of rats treated with YQHG was reshaped, which was characterized by a reduced ratio of Firmicutes/Bacteroidota.

Conclusion: Our results predicted and verified the potential targets of YQHG on CKD from a holistic perspective, and provided valuable direction for the further research of YQHG.

Keywords: Yishen Qingli Heluo granule, network pharmacology, chronic kidney disease, 5/6 nephrectomy, gut microbiota

Introduction

Chronic kidney disease (CKD) is increasingly recognized as a global public health issue with high morbidity (8724 per 100,000 people) and mortality (15.9 per 100,000 people).[1] The risk factors and disease pathways that lead to compromised kidney function are diverse and poorly clarification. Consequently, few strategies are available to delay the progression of CKD, with most current treatment strategies centred around reducing proteinuria, lowering blood pressure and uric acid. For instance, renin-angiotensin system inhibitors are the main therapeutic drugs for the treatment of CKD

Received: 16 November 2021
Accepted: 9 March 2022
Published: 24 March 2022

in terms of reducing proteinura and protecting kidney function.[2,3] However, study reported that these drugs may not help prevent the progression of CKD to end-stage kidney disease (ESRD);[4] moreover, they might cause a series of side effects, such as increased serum potassium, creatinine, and cancer risk.[5–8] At present, the number of people receiving kidney replacement therapy has exceeded 2.6 million and is expected to double to 5.4 million worldwide by 2030.[9] Once CKD progresses to ESRD, it will not only bring economic burden to patients, but also affect their quality of life to a great extent. Accordingly, there is an urgent need to explore potential therapeutic drugs to prevent and treat CKD in this field.

Traditional Chinese Medicine (TCM) has been recognized as potential treatment option for CKD because of its proven effectiveness, wide range of applications, and few side effects. Many cases have shown that TCM herbs is regarded as an alternative source for delaying the progression of CKD due to conventional experience and multi-target characteristics.[10–12] Yishen Qingli Heluo granule (YQHG) was independently developed by Jiangsu Province Hospital of Chinese Medicine as TCM remedy for the clinical treatment of CKD. The clinical studies had demonstrated that YQHG could improve the clinical symptoms and reduce the level of serum creatinine (Scr). Moreover, the progression of CKD3 to CKD4 could also be delayed by YQHG.[13,14] Our previous study showed that YQHG could attenuate kidney injury by regulating autophagy, apoptosis and inflammatory response.[15] However, most studies on the granule mainly centred around some classic signaling pathways such as MAPK, TGF-β and related pathways, which was lack of comprehensiveness. Due to the absence of effective systematic methods in the past, the research on the effective compounds, targets and corresponding pharmacological mechanisms of YQHG against CKD is limited. Hence, the researches have been focused on the mechanism of a monomer or active compound of YQHG in treating CKD. However, YQHG is like a sophisticated orchestra of various instruments. How these 10 herbs work together to play the perfect repertoire still needs to be explored. Therefore, it's important to find novel avenues to comprehensively understand the mechanisms of YQHG against CKD. Network pharmacology is a cutting-edge methodology, which is first proposed by Hopkins.[16] This method is consistent with the holistic view of TCM. In recent years, it has been widely used to elucidating the mechanisms of TCM in the treatment of chronic disease, including CKD.[17–19]

In this study, we first used the network pharmacology approach as a tool to explore the active compounds of YQHG and investigate its underlying mechanism of action in the treatment of CKD. Then, molecular docking was used to verify the reliability of network pharmacology. In addition, we validated the nephroprotective potential of YQHG and key targets expressions in 5/6 nephrectomized rats. It's worth noting that previous studies had shown that the gut microbiota played an important role in the therapeutic effect of TCM.[20–22] The gut microbiota could change the chemical composition of TCM herbs to make it had a different bioavailability, biological activity or toxicity than the precursor. TCM herbs could also reshape the diversity and composition of gut microbiota to alleviate related disease.[23] Hence, 16S rRNA sequencing is used to analyze the relationship among TCM herbs, CKD and the profile of gut microbiota, laying the foundation for further research on YQHG. The details of the analysis process of this research are shown in Figure 1.

Materials and Methods

Network Pharmacology Analyses

Acquiring of Active Compounds and Related Targets in YQHG

Compounds of the each herb in YQHG were obtained from TCMSP database (https://old.tcmsp-e.com/tcmsp.php) and wide-scale literature mining. The compounds were filtered through the ADME evaluation system, in which oral bioavailability (OB) and drug-likeness (DL) were the main parameters. OB≥30% and DL≥0.18 were the thresholds values of ADME filtering method recommended by TCMSP database.[24] TCMSP, STITCH (http://stitch.embl.de/), PubChem (https://pubchem.ncbi.nlm.nih.gov/) and Swiss Target Prediction (http://www.swisstargetprediction.ch/) databases were utilized to identify the targets corresponding to each active compound in YQHG. The Uniprot (https://www.uniprot.org/) database was used to standardize the results.

Fishing for Candidate Targets of YQHG in Treating CKD

Targets related to CKD were acquired from GeneCards (https://www.genecards.org/), OMIM (http://www.omim.org/), DisGeNET (https://www.disgenet.org/), TTD (http://db.idrblab.net/ttd/) and MalaCards (https://www.malacards.org/) databases. All the collected targets of CKD and YQHG were merged after being standardized by Uniprot database.

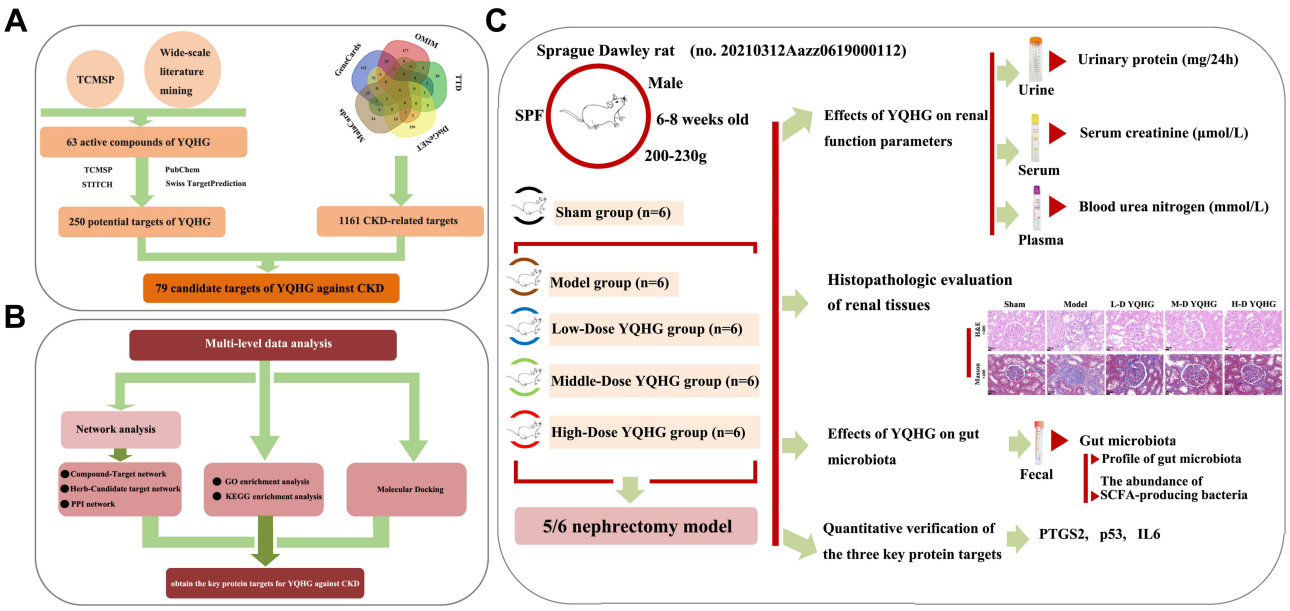

Figure 1 The work flow of the study. (**A**) Compounds screening and targets fishing. (**B**) Multi-level data analysis. (**C**) Experimental validation.

The candidate targets of YQHG against CKD were identified by the Venn platform (http://bioinformatics.psb.ugent.be/webtools/Venn/), and the results were used for further analysis.

Network Construction

(1) Compound-target (C-T) network of YQHG: The data of active compounds and their corresponding targets were imported into Cytoscape software (v3.6.0, Boston, MA, USA) to construct the C-T interaction network. The degree centrality, betweenness centrality and closeness centrality were evaluated by Network Analyzer plug-in of Cytoscape software. According to the three topological parameters of each node, the key active compound of YQHG were selected and analyzed. (2) Herb-Candidate target (H-CT) network of YQHG: The data of 10 herbs and candidate targets were imported into Cytoscape software to construct the H-CT interaction network. The pie chart was used to indicate the herb to which the candidate target (represented by circular nodes) belonged. (3) Protein-protein interaction (PPI) network of candidate targets: The visualization of PPI network was obtained by combining STRING database (https://string-db.org/) and Cytoscape software. The species were limited to Homo sapiens, and the PPI confidence score>0.9 was the filtering parameter recommended by STRING database.[25] Nodes and edges represent candidate targets and protein-protein interactions in the PPI network, respectively. In this study, the core target proteins were selected and identified by the parameter " Degree ". Degree was used to evaluate the topological importance of the nodes in the network, which was calculated by Network Analyzer plug-in of Cytoscape software.

GO and KEGG Pathway Enrichment Analysis

In order to investigate the key terms of GO biological process and critical signaling pathways of candidate targets, the R package (clusterProfiler, version 4.1.0) was used for GO and KEGG enrichment analysis.[26] Adjusted P value<0.05 was considered statistically significant.

Molecular Docking

In the study of molecular docking, Autodock Vina 1.1.2 software was used to determine the binding mode and interactions between the key active compounds of YQHG and hub proteins identified based on PPI and network analyzer analyses. This approach involved the following main steps: (1) Ligand molecule preparation. The 3D structures of active compounds were download in mol2 format from TCMSP database. AutodockTools 1.5.6 was used to open the ligand molecule, add hydrogen, gasteiger charge, detection of ligand root, search and definition of rotatable bond, and finally save it in pdbqt format. (2) Receptor molecule preparation. The 3D structures of hub proteins were download from RCSB

Protein Data Bank (www.rcsb.org). AutodockTools 1.5.6 was used to upload the protein. After adding all hydrogen atoms, calculating gasteiger charge and combining non-polar hydrogen, it is defined as the receptor and saved as pdbqt format. (3) Setting of docking parameters. AutoGrid tool to set the parameters of the docking box (X-Y-Z coordinates and grid size). In order to increase the accuracy of calculation, the exhaustiveness value was set to 20. (4) Execution and output. Autodock Vina 1.1.2 software was used for semi flexible docking, and the best conformation was selected as the final docking conformation. (5) Analysis and visualization. The conformation with the best binding affinity was selected for docking mode analysis. The binding affinity of the protein was less than −5 kcal/mol, suggesting that the protein had a certain binding activity with the compound.[27] The docking results of compound and protein with the best conformation were analyzed and visualized by PyMol software.

Preparation of YQHG

YQHG (batch number 20051031) was composed of 10 single TCM granules: Angelicae Sinensis Radix (Danggui, DG), Achyranthis Bidentatae Radix (Niuxi, NX), Centella Asiatica (L.) Urban (Jixuecao, JXC), Polygonati Rhizoma (Huangjing, HJ),Smilacis Glabrae Rhixoma (Tufuling, TFL), Radix Rhei Et Rhizome (Dahuang, DH), Pyrrosiae Folium (Shiwei, SW), Hedysarum Multijugum Maxim (Huangqi, HQ), Serissa Japonica (Thunb.) Thunb (Liuyuexue, LYX), Polygoni Cuspidati Rhizoma Et Radix (Huzhang, HZ), which was manufactured by Jiangyin Tianjiang Pharmaceutical Co., Ltd. (Wuxi, Jiangsu, China). The ratios of the single TCM granule to the corresponding crude drug were listed in Table 1. All the above granules were authenticated by Professor Wei Sun (Nanjing University of Chinese Medicine, Nanjing, Jiangsu, China). The weight-based drug dosing format (per kg) was used in this study to calculate the YQHG doses in rats.[28] Calculated with an adult body weight of 70 kg, the clinical equivalent dose converted into rats was 2.8g/kg, which was used as the medium dose of YQHG. The low dose and high dose in this study were half and twice the medium dose of YQHG, respectively. UHPLC-MS was conducted to confirm the stability and effectiveness of YQHG extract.

Construction of 5/6 Nephrectomy and YQHG Administration

Male Sprague Dawley (SD) rats (no. 20210312Aazz0619000112, 6–8 weeks old, 200–230g) were provided by Vital River Experimental Animal Co., Ltd. (Zhejiang, China). Rats were housed in a specific pathogen-free experimental animal center of Nanjing University of Chinese Medicine. Specifically, rats were housed in plastic cages and provided with sufficient standard food and water freely. The environmental conditions of the room where the rats were raised included temperature (22±2°C), humidity (50±10%), and 12/12 hour light/dark cycle. All animal experiments were performed according to the protocol approved by Animal Care and Use Committee of Nanjing University of Chinese Medicine [permission number 202101A047]. The guidelines followed for the welfare of the laboratory animals was Laboratory Animal Guidelines for Ethical Review of Animal Welfare (GB/T 35892–2018). All surgeries were performed under appropriate anesthesia, and every efforts were made to minimize animal suffering.

CKD was induced in 24 rats by a two-step 5/6 nephrectomy as previously described.[29] The procedure of the two operations was as follows: ablated 2/3 of the left kidney parenchyma (avoid the kidney hilum), and then quickly placed a gelatin sponge on the incision surface to stop bleeding for 4–5 minutes. One week later, a right-sided unilateral nephrectomy was performed. The kidney pedicle was ligated with a sterile 3–0 suture, and then the right kidney was resected. The abdominal cavity was flushed with 0.9% sterile saline to avoid postoperative abdominal adhesion after two surgical operations. Induction and maintenance of anesthesia (consumption of Isoflurane was 6mL/h and 3mL/h, respectively) during the operation were carried out with the Rodent Gas Anesthesia Machine (Yuyan-ABS). Six rats underwent sham operation were used as control. CKD rats were randomly divided into four groups (n=6 for each group). The subgroups and the daily dose of gavage substances were as follows: I) Model group (sterile water); II Low-Dose YQHG group (1.4g/kg YQHG); III) Middle-Dose YQHG (2.8g/kg YQHG); IV) High-Dose YQHG (5.6g/kg YQHG). During the experiment, all rats were weighed twice a week, and the drug doses were adjusted accordingly. At the end of the experiment, urine and fecal samples were collected from rats before sacrificed. Blood samples and kidney tissues were collected for further studies.

Table 1 Details of YQHG

Herb Name	Latin Name	Family	Genus	Parts Used	Amount Used (g)	Ratio
Danggui	Angelicae Sinensis Radix	Umbelliferae	Angelica L.	Root	4	2:5
Niuxi	Achyranthis Bidentatae Radix	Amaranthaceae	Achyranthes L.	Root	3	3:10
Jixuecao	Centella Asiatica (L.) Urban	Umbelliferae	Centella L.	Herba	3	1:10
Huangjing	Polygonati Rhizoma	Liliaceae Juss.	Polygonatum Mill.	Rhizome	8	2:5
Tufuling	Smilacis Glabrae Rhixoma	Liliaceae	Smilax L.	Rhizome	2	1:15
Dahuang	Radix Rhei Et Rhizome	Polygonaceae	Rheum L.	Rhizome	2	1:3
Shiwei	Pyrrosiae Folium	Polypodiaceae	Pyrrosia Mirbel.	Leave	2	1:10
Huangqi	Hedysarum Multijugum Maxim	Leguminosae sp.	Astragalus Linn.	Root	4.5	3:20
Liuyuexue	Serissa Japonica (Thunb.) Thunb	Rubiaceae Juss.	Serissa Comm. ex Juss.	Whole plant	1	1:30
Huzhang	Polygoni Cuspidati Rhizoma Et Radix	Polygonaceae	Reynoutria Houtt.	Rhizome, Root	1	1:15

https://doi.org/10.2147/DDDT.S348335

Reagents

Scr, blood urea nitrogen (BUN) and urinary protein quantification assay kits (C011-2-1, C013-2-1, C035-2-1) were purchased from Nanjing Jiancheng Biotech Co., Ltd. (Nanjing, Jiangsu, China). IL-6 ELISA kit (bsk00042) was purchased from Nanjing Jinyibai Biotech Co., Ltd. (Nanjing, Jiangsu, China). BCA protein concentration assay kit (PC0020) was obtained from Beijing Solarbio Science & Technology Co., Ltd. (Beijing, China). Anti-PTGS2 antibody (ab179800), Anti-p53 antibody (ab227655), Anti-GAPDH antibody (ab181602) and Goat Anti-Rabbit IgG H&L (HRP) (ab6721) were purchased from Abcam (Cambridge, UK).

Scr, BUN and 24h Urinary Protein Quantification

Scr, BUN and 24h urinary protein levels were measured using Scr, BUN and urinary protein quantification assay kits according to the instructions. Among them, urinary protein quantification was undertaken by 24h urine collection with metabolic cages on the day before the rats were sacrificed. The formula is as follows: Urinary protein (mg/24h) = urinary protein concentration (mg/L)×24h urine volume (L).

Histopathologic Evaluation of Kidney Tissues

Rat kidneys were rinsed with precooled PBS (Solarbio) and then fixed in 4% paraformaldehyde (biosharp). Sections (4μm) were cut from paraffin-embedded kidney tissue and stained with hematoxylin and eosin (H&E) or Masson's trichrome (Masson) (Solarbio). Light microscope images were photographed using a Digital Slide Scanner (Type specification: Pannoramic DESK, P-MIDI, P250; Company: 3D HISTECH; Country: Hungary; Scanning software: Pannoramic Scanner). The steps for calculating the area of glomerular and tubulointerstitial fibrosis were as follows: First of all, CaseViewer2.4 software was used to select the glomerular (tubulointerstital) area for 40×imaging. Try to fill the entire field of view with the tissue, and ensure that the background light of each image was consistent. Secondly, Image-Pro Plus 6.0 software performed image analysis, set pixel as the standard unit, and two fields of view were selected for each slice. Finally, the fibrosis area was evaluated, that was, the percentage of fibrosis area (%) = glomerular (tubulointerstital) fibrosis area/glomerular (tubulointerstital) area×100%.

Gut Microbiota Analysis

Feces of all rats in the five groups (Sham, Model, L-D YQHG, M-D YQHG, H-D YQHG) were collected for gut microbiota analyses. The four main steps involved in the sequencing of gut microbiota were as follows: I) Extraction of genome DNA: The total DNA of feces were extracted by E.Z.N.A.® Soil DNA Kit (Omega Bio-tek) according to manufacturer' s protocols. DNA concentration and purity were monitored on 1% agarose gel. II) PCR amplification: The V3-V4 region of 16S rRNA gene was amplified using specific primer (338F_806R) with the barcode. The PCR amplification was carried out using TransStart Fastpfu DNA polymerase kit. III) PCR products quantification, mixing and purification: Refer to the preliminary quantification results of electrophoresis, QuantiFluor™ -ST Assay Kit (Promega) was used to detect and quantify the PCR products, and then mix the corresponding proportions according to the sequencing requirements of each sample. Then, the mixture of PCR products was purified with GeneJET Gel Extraction Kit (Thermo Fisher Scientific). IV) Library preparation and sequencing: The profiling was carried out on the MiSeq platform (Illumina, Inc., San Diego, CA). Fast Length Adjustment of Short reads (FLASH, Version 1.2.11) was used to filter 16S rRNA sequencing data. Operational taxonomic units (OTUs) were picked at a 97% similarity cut-off, and the purified amplicons were sequenced on an Illumina MiSeq platform at Majorbio Biopharm Technology Co. Ltd. (Shanghai, China) according to the standard protocols.

Western Blot and ELISA

The total protein of frozen kidney samples was extracted with RIPA lysis buffer (Beyotime) containing 1% PMSF (Beyotime). Protein concentration was determined by BCA protein concentration assay kit (Solarbio) according to the instructions. Proteins were separated by SDS-PAGE gels and transferred onto PVDF membranes (Solarbio). After blocking with 5% BSA (Solarbio), the membranes were incubated with primary antibodies PTGS2 (1:1000), p53 (1:1000), GAPDH (1:10,000) at 4°C overnight. Subsequently, the membranes were washed with TBST (Solarbio) and

incubated for 60 minutes at room temperature with Goat Anti-Rabbit IgG H&L (HRP) (1:20,000). The membranes were incubated with Ultrasensitive ECL Detection Kit (Proteintech) for 1–2 minutes, and then detected on the BIO-RAD ChemiDoc XRS+ Gel Imaging System (Bio-Rad, California, USA). The gray values of the protein bands were analyzed using the Image Lab software (Bio-Rad).

PBS was added to the kidney tissue (1mL/0.1g), and electro-homogenized sample was centrifuged to collect the supernatant. Subsequently, the rat IL-6 ELISA kit was used to detect the expression of IL-6 according to the instructions.

Statistical Analysis

All data were expressed as mean±SEM. GraphPad Prism 9.0 software (GraphPad, CA, USA) was used for statistical analysis and image construction. We combined QQ plots (Supplementary Figure 1) with the Shapiro–Wilk test to assess data normality. For normally distributed data, one-way ANOVA followed by Tukey's test was used. For non-normally distributed data, Kruskal–Wallis test followed by non-parametric Wilcoxon rank-sum test was used. $p<0.05$ was considered statistically significant.

Results

Information on Active Compounds and Related Targets of YQHG

A total of 63 active compounds of YQHG were selected from the TCMSP database and wide-scale literature mining. All active compounds satisfied the ADME filtering method, OB≥30% and DL≥0.18. The numbers of compounds for each herb in YQHG were 17 (NX), 13 (TFL), 16 (HQ), 10 (HZ), 10 (DH), 8 (HJ), 5 (SW), 2 (DG), 2 (JXC), 1 (LYX) (Table S1). Among the 63 active compounds, there were 9 compounds that existed in more than one herb. For example, compound Quercetin could be found in 6 herbs (HQ, NX, HZ, TFL, SW, JXC) of YQHG.

We identified 250 targets for 63 active compounds (Table S2). The number of potential targets affected by active compounds from HQ, NX, HZ, TFL, SW, JXC, HJ, DH, DG, and LYX were 208, 201, 193, 174, 169, 150, 55, 43, 30 and 11, respectively. Many active compounds exerted their pharmacological effects through binding to more than one target simultaneously. For instance, wogonin, as an active compound in NX, can interact with 43 targets, including TP53, CASP3, PTGS2, IL-6 and so on.

Candidate Targets of YQHG Against CKD

Through databases screening, 1161 CKD-related targets were obtained (526 in OMIM database, 379 in DisGeNET database, 331 in GeneCards database, 113 in MalaCards database, and 73 in TTD database). The intersection targets were shown by a Venn diagram (Figure 2A).

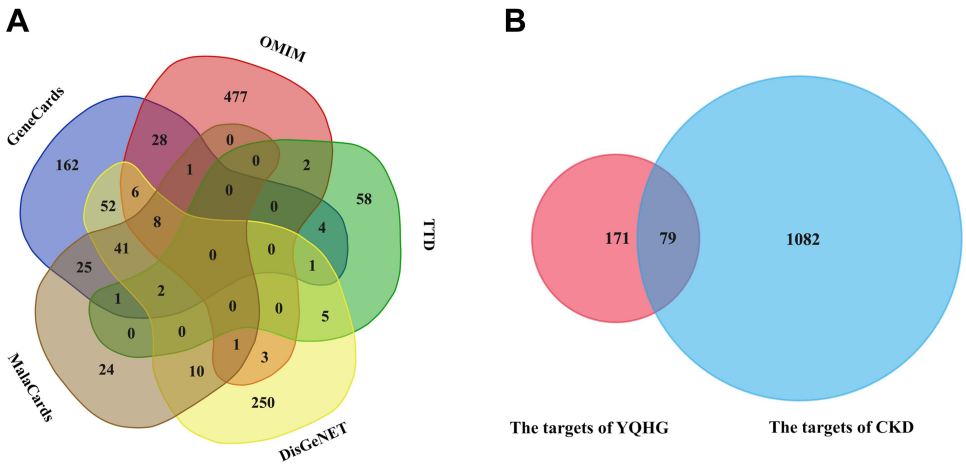

Figure 2 Venn diagrams. (**A**) The targets of CKD. CKD-related targets obtained from five databases (OMIM, DisGeNET, GeneCards, MalaCards, TTD). (**B**) Candidate targets of YQHG in the treatment of CKD.

The potential targets of YQHG were overlapped with CKD-related targets by the Venn platform (Figure 2B). A total of 79 intersecting targets were selected as candidate targets for YQHG against CKD (Table 2). Herein, we investigated the distribution of CKD relevant targets among the 10 herbs (72 from HQ, 72 from HZ, 69 from NX, 64 from SW, 64 from TFL, 59 from JXC, 21 from HJ, 15 from DH, 9 from DG, 2 from LYX) via a Venn analysis. These 79 targets were then used to construct H-CT network by Cytoscape.

Network Visualization

(1) C-T network. In order to reveal the synergistic effects of multi-compound and multi-target in the 10 herbs of YQHG (Figure 3A) and evaluate its mechanism of action, a C-T network analysis was carried out (Figure 3B). The

Table 2 Candidate Targets of YQHG in the Treatment of CKD

Uniprot	Gene Symbol	Protein Name	Uniprot	Gene Symbol	Protein Name
Q9UNQ0	ABCG2	ATP-binding cassette sub-family G member 2	P22301	IL10	Interleukin-10
P00326	ADH1C	Alcohol dehydrogenase 1C	P01583	IL1A	Interleukin-1 alpha
P07550	ADRB2	Beta-2 adrenergic receptor	P01584	IL1B	Interleukin-1 beta
P31749	AKT1	RAC-alpha serine/threonine-protein kinase	P60568	IL2	Interleukin-2
P05067	APP	Amyloid beta A4 protein	P05112	IL4	Interleukin-4
P10275	AR	Androgen Receptor	P05231	IL6	Interleukin-6
Q07812	BAX	Apoptosis regulator BAX	P06213	INSR	Insulin receptor
P10415	BCL2	Apoptosis regulator Bcl-2	P35968	KDR	Vascular endothelial growth factor receptor 2
P42574	CASP3	Caspase-3	P28482	MAPK1	Mitogen-activated protein kinase 1
Q14790	CASP8	Caspase-8	Q00987	MDM2	E3 ubiquitin-protein ligase Mdm2
P04040	CAT	Catalase	P08581	MET	Hepatocyte growth factor receptor
Q03135	CAV1	Caveolin-1	P03956	MMP1	Interstitial collagenase
P13500	CCL2	C-C motif chemokine 2	P08253	MMP2	72 kDa type IV collagenase
P24385	CCND1	G1/S-specific cyclin-D1	P14780	MMP9	Matrix metalloproteinase-9
P29965	CD40LG	CD40 ligand	P05164	MPO	Myeloperoxidase
P38936	CDKN1A	Cyclin-dependent kinase inhibitor 1	P14598	NCF1	Neutrophil cytosol factor 1
P42771	CDKN2A	Cyclin-dependent kinase inhibitor 2A, isoforms 1/2/3	Q16236	NFE2L2	Nuclear factor erythroid 2-related factor 2
P11229	CHRM1	Muscarinic acetylcholine receptor M1	P35228	NOS2	Nitric oxide synthase, inducible
P20309	CHRM3	Muscarinic acetylcholine receptor M3	P29474	NOS3	Nitric oxide synthase, endothelial
P08912	CHRM5	Muscarinic acetylcholine receptor M5	P08235	NR3C2	Mineralocorticoid receptor
P02452	COL1A1	Collagen alpha-1(I) chain	P27169	PON1	Serum paraoxonase/arylesterase 1
P02741	CRP	C-reactive protein	P37231	PPARG	Peroxisome proliferator-activated receptor gamma
P27487	DPP4	Dipeptidyl peptidase IV	O14684	PTGES	Prostaglandin E synthase
P01133	EGF	Pro-epidermal growth factor	P23219	PTGS1	Prostaglandin G/H synthase 1
P00533	EGFR	Epidermal growth factor receptor	P35354	PTGS2	Prostaglandin G/H synthase 2
P04626	ERBB2	Receptor tyrosine-protein kinase erbB-2	Q04206	RELA	Transcription factor p65
P03372	ESR1	Estrogen receptor	Q13950	RUNX2	Runt-related transcription factor 2
P00734	F2	Thrombin	Q96EB6	SIRT1	NAD-dependent deacetylase sirtuin-1
P02751	FN1	Fibronectin	Q01959	SLC6A3	Sodium-dependent dopamine transporter
P17302	GJA1	Gap junction alpha-1 protein	P31645	SLC6A4	Sodium-dependent serotonin transporter
P09488	GSTM1	Glutathione S-transferase Mu 1	P03973	SLPI	Antileukoproteinase
P09211	GSTP1	Glutathione S-transferase P	P00441	SOD1	Superoxide dismutase [Cu-Zn]
Q16665	HIF1A	Hypoxia-inducible factor 1-alpha	P10451	SPP1	Osteopontin
P09601	HMOX1	Heme oxygenase 1	P42224	STAT1	Signal transducer and activator of transcription 1-alpha/beta
P04792	HSPB1	Heat shock protein beta-1	P07204	THBD	Thrombomodulin
P28223	HTR2A	5-hydroxytryptamine 2A receptor	P04637	TP53	Cellular tumor antigen p53
P05362	ICAM1	Intercellular adhesion molecule 1	P19320	VCAM1	Vascular cell adhesion protein 1
P01579	IFNG	Interferon gamma	P15692	VEGFA	Vascular endothelial growth factor A
P11717	IGF2	Insulin-like growth factor II	P47989	XDH	Xanthine dehydrogenase/oxidase
P17936	IGFBP3	Insulin-like growth factor-binding protein 3			

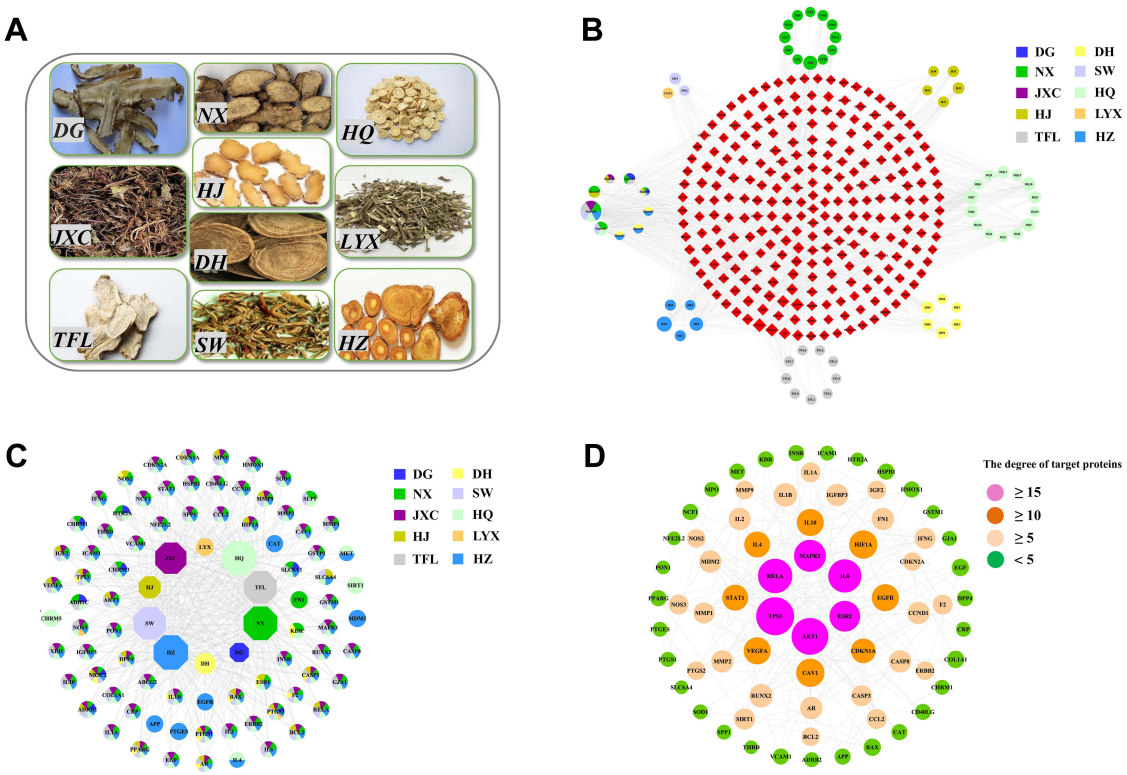

Figure 3 Network visualization. (**A**) The 10 herbs of YQHG. (**B**) C-T network of YQHG. The C-T network is constructed by the active compounds (circle) and their corresponding potential targets (rhombus). (**C**) H-CT network of YQHG. The 79 candidate targets (circles) of YQHG against CKD are connected with their corresponding herbs (octagons). The color of the target represents their corresponding herbs. (**D**) PPI network of candidate targets.

active compounds corresponding to the abbreviations in Figure 3 were shown in Table S1. The C-T network consisted of 63 active compounds, 250 targets, and 914 C-T interactions (313 nodes and 914 edges). The average degree centrality, betweenness centrality, and closeness centrality values were 14.67, 0.02, and 0.33, respectively. The above topological parameters of 12 compounds were higher than the average, which were shown in Table 3. These compounds were considered to be the main active compounds of YQHG in the treatment of CKD. The average number of targets for each herb was 123, indicating the multi-target properties of these herbs. A total of 31 key targets satisfied the screening rules (degree centrality>3.656, betweenness centrality>0.003, closeness centrality>0.333), of

Table 3 The Topological Parameter Analysis of Top 12 Compounds in YQHG

Number	Compound	Degree Centrality	Betweenness Centrality	Closeness Centrality
1	Quercetin	150	0.513	0.527
2	Kaempferol	61	0.122	0.412
3	Luteolin	55	0.105	0.393
4	7-O-methylisomucronulatol	44	0.066	0.385
5	Wogonin	43	0.055	0.378
6	Stigmasterol	30	0.064	0.375
7	Baicalein	35	0.078	0.374
8	Isorhamnetin	34	0.037	0.374
9	Physovenine	37	0.045	0.372
10	Formononetin	38	0.051	0.371
11	Hederagenin	23	0.044	0.368
12	Aloe-emodin	22	0.025	0.362

which PTGS2 has the highest filtering parameters (degree centrality=41, betweenness centrality=0.085, closeness centrality=0.516). (2) H-CT network. To explore the synergistic effects of YQHG at the individual herb level, we constructed a H-CT network (Figure 3C). We found that 6 herbs covered more than 75% of the 79 candidate targets, of which HQ and HZ both covered 91%. Interestingly, the 10 herbs in YQHG shared a common target, which is PTGS2. The existence of this target is a manifestation of the synergistic effect of TCM, which may be involved in the pathological process of CKD. (3) PPI network. The proteins with combined score>0.90 were chosen to construct PPI network (Figure 3D). The parameter "Degree" was used to evaluate the topological importance of the nodes in the network. The top 6 proteins obtained by the network analyzer in Cytoscape software were TP53, AKT1, RELA, IL6, MAPK1 and ESR1. Subsequently, the top 6 active compounds (Quercetin, Kaempferol, Luteolin, 7-O-methylisomucronulatol, wogonin, Stigmasterol) and six protein targets screened through the C-T and PPI networks were used for further analysis.

GO and KEGG Enrichment Analysis

GO terms were classified according to biological process, molecular function and cellular component, and the top 10 were shown in Figure 4A. Candidate target proteins of molecular function category were mostly associated with receptor activator activity and receptor ligand activity. Target proteins in cellular component category were enriched in membrane microdomain and membrane raft. As for GO biological process, it played a major role in the above three GO terms. Therefore, clarifying the relevant biological process of YQHG against CKD pointed out the direction for the mechanism to a certain extent. According to 79 candidate targets of YQHG in the treatment of CKD, top 10 biological processes were identified. They focused on two areas: (1) Regulation of cell cycle and apoptosis (epithelial cell proliferation, regulation of apoptotic signaling pathway, negative regulation of apoptotic signaling pathway). (2) Regulation of reactive oxygen species (ROS) metabolic process (response to oxidative stress, reactive oxygen species metabolic process, response to oxygen levels, cellular response to oxidative stress, response to reactive oxygen species, regulation of reactive oxygen species metabolic process, positive regulation of reactive oxygen species metabolic process). To further elucidate the potential mechanisms of YQHG against CKD, we screened top 40 KEGG pathways by clusterProfiler (Figure 4B). The results showed that 8 important signaling pathways (p53, Toll-like receptor, VEGF, T cell receptor,

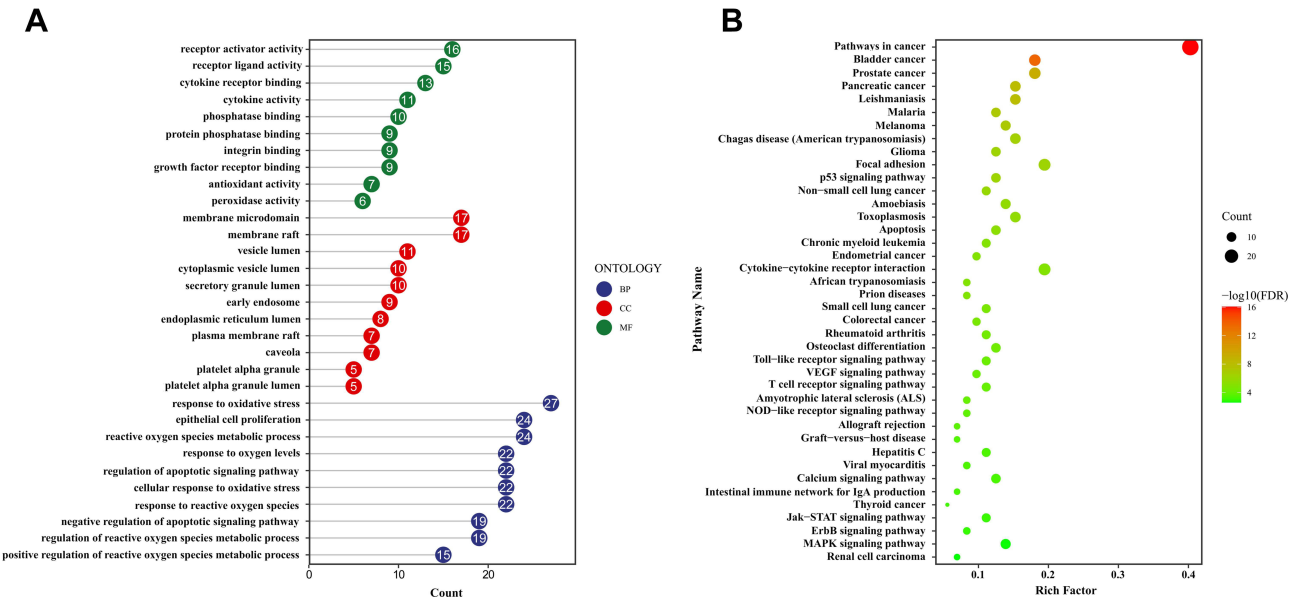

Figure 4 GO and KEGG enrichment analysis for candidate targets of YQHG against CKD. (**A**) GO enrichment analysis. GO terms are classified according to biological process (BP), molecular function (MF) and cellular component (CC). The top 10 terms of each one are presented. (**B**) KEGG enrichment analysis. The top 40 KEGG signaling pathways are presented. The X-axis represents the rich factor, bubble size represents the count of targets enriched in terms and the color represents the p value.

Nod-like receptor, Calcium, JAK-STAT, MAPK) were identified as CKD-related target pathways, and p53 was considered to be the most critical one.

Molecular Docking of Core Active Compounds and Proteins

To further verify the accuracy of network pharmacology, the binding affinity between key active compounds and hub proteins was analyzed by molecular docking method based on Autodock Vina software. The binding affinity of the six active compounds (Quercetin, Kaempferol, Luteolin, 7-O-methylisomucronulatol, Wogonin, Stigmasterol) to hub proteins (TP53, AKT1, RELA, IL6, MAPK1, ESR1) were all less than −5 kcal/mol, indicating that they possessed good binding activity. The details of the binding affinity were shown in Table 4. Hydrogen bonding plays a critical role in stabilizing compound-protein bonding interactions. Therefore, the favorable bond distance between H-donor and H-acceptor atoms is ensured to be less than 3.5 Å [24]. Quercetin, Kaempferol and Luteolin were the best in the binding mode with six proteins in present study. Moreover, an UHPLC-MS approach was established to reveal the stability of YQHG (Figure S2A and B) and quantify the key active compounds (Quercetin, Kaempferol and Luteolin) in the extract (Table S3, and Figure S2C and D). The docking results of compound and protein with the best conformation were shown in Figure 5.

YQHG Improved Kidney Function and Fibrosis in 5/6 Nephrectomized Rats

A comprehensive assessment of kidney appearance (colour, capsule, border), related parameters (Scr, BUN, urinary protein, glomerular fibrosis area, tubulointerstitial fibrosis area), and kidney tissue pathology (H&E, Masson) were conducted to explore the potential therapeutic value of YQHG on CKD. To this end, 5/6 nephrectomy model and YQHG dosing regimen was established (Figure 6A). As expected, the model group exhibited weight loss, pale kidneys, uneven borders, and a hard-to-peel capsules. Remarkably, treatment with YQHG in a dose-dependent manner impeded disease progression, which was shown by increased body weight of rats, recovery of reddish-brown kidneys, integrity of borders, and smoothness of the capsules (Figure 6B and C). Scr, BUN, and urinary protein are the key markers indicating the kidney dysfunction. Our results showed that compared with the model group, YQHG significantly reduced the levels of the three parameters in a dose-dependent manner (Figure 6D–F). Histopathological analysis clearly showed inflammation infiltration, mesangial expansion, tubular atrophy and dilation, glomerular sclerosis, and interstitial fibrosis in 5/6 nephrectomy rats, all of which were dramatically ameliorated by YQHG treatment (Figure 6G). In addition, histopathological indicators including glomerular fibrosis area and tubulointerstitial fibrosis area were examined upon YQHG treatment. Here, we found YQHG treatment significantly decreased the glomerular fibrosis area (Figure 6H). Moreover, H-D YQHG treatment significantly decreased tubulointerstitial fibrosis area (Figure 6I). Taken together, these data indicated that YQHG had a profound protective effect on 5/6 nephrectomized rats, which was characterized by alleviating tissue damage, improving kidney function and reducing kidney fibrosis.

YQHG Reshaped Gut Microbiota by Reducing Firmicutes/Bacteroidota Ratio in 5/6 Nephrectomized Rats

TCM herbs interact closely with gut microbiota and affect their composition.[30] On the contrary, the gut microbiota also plays an important role in converting carbohydrates, proteins, lipids and small non-nutritive chemicals from TCM herbs into chemical metabolites that may have beneficial or adverse effects on human health.[31] Given that gut microbiota homeostasis plays an important role in the efficacy of TCM herbs,[32–34] we then investigated the effects of YQHG on gut microbiota in 5/6 nephrectomized rats. We analyzed gut microbiota at two different taxonomic levels (phylum and genus). PCoA revealed that the gut microbial composition of the YQHG groups was close to that of the sham group and distinct from that of the model group (Figure 7A and F). The community analysis at the phylum level showed that compared with the sham group and the YQHG groups (Figure 7B), the gut microbial composition of the model group changed in certain bacteria, such as Firmicutes and Bacteroidota. Specifically, L-D YQHG treatment significantly reduced the abundance of Firmicutes (Figure 7C) and increased the abundance of Bacteroidota (Figure 7D). Importantly, the ratio of these two bacteria was significantly reduced by YQHG treatment in a dose-

Table 4 The Binding Affinity Between Active Compounds and Hub Proteins

PDB ID	Proteins	Affinity (kcal/mol)					
		Quercetin	Kaempferol	Luteolin	7-O-methylisomucronulatol	Wogonin	Stigmasterol
6SI3	TP53	−7.14	−7.27	−7.84	−6.98	−7.28	−5.45
4GV1	AKT1	−7.52	−7.83	−7.16	−6.49	−7.08	−5.68
1VJ7	RELA	−7.79	−7.65	−7.41	−6.81	−6.95	−5.64
1BQU	IL6	−7.29	−7.22	−7.19	−6.81	−6.66	−5.71
4QP2	MAPK1	−7.90	−7.63	−7.69	−6.56	−6.87	−6.08
7KCD	ESR1	−7.79	−7.73	−8.48	−7.17	−7.29	−6.01

dependent manner (Figure 7E). Moreover, the gut microbiota at the genus level was reshaped in the YQHG groups, which was shown by community barplot and Circos plot (Figure 7G and H). Taken together, these results demonstrated that YQHG treatment effectively restored the composition of the gut microbiota and reduced the ratio of Firmicutes/Bacteroidota (F/B), thereby promoting the normalization of gut microbial ecosystem in order to exert the curative effect of TCM herbs.

YQHG Regulated the Expression of PTGS2, P53 and IL-6 in 5/6 Nephrectomized Rats

H-CT network, KEGG pathway enrichment analysis and molecular docking predicted that three key protein targets (PTGS2, p53, IL6) were involved in YQHG against CKD. Therefore, the expressions of PTGS2 and p53 were examined upon YQHG treatment. Here, we found H-D YQHG treatment significantly decreased the expression of PTGS2 in kidney tissue (Figure 8A and B). Moreover, H-D YQHG could regulate the expression of p53 to a certain extent (Figure 8A and C). Next, we evaluated the inhibitory effect of YQHG on IL6 expression. After YQHG treatment, the expression of IL6 was significantly decreased in kidney tissue (Figure 8D).

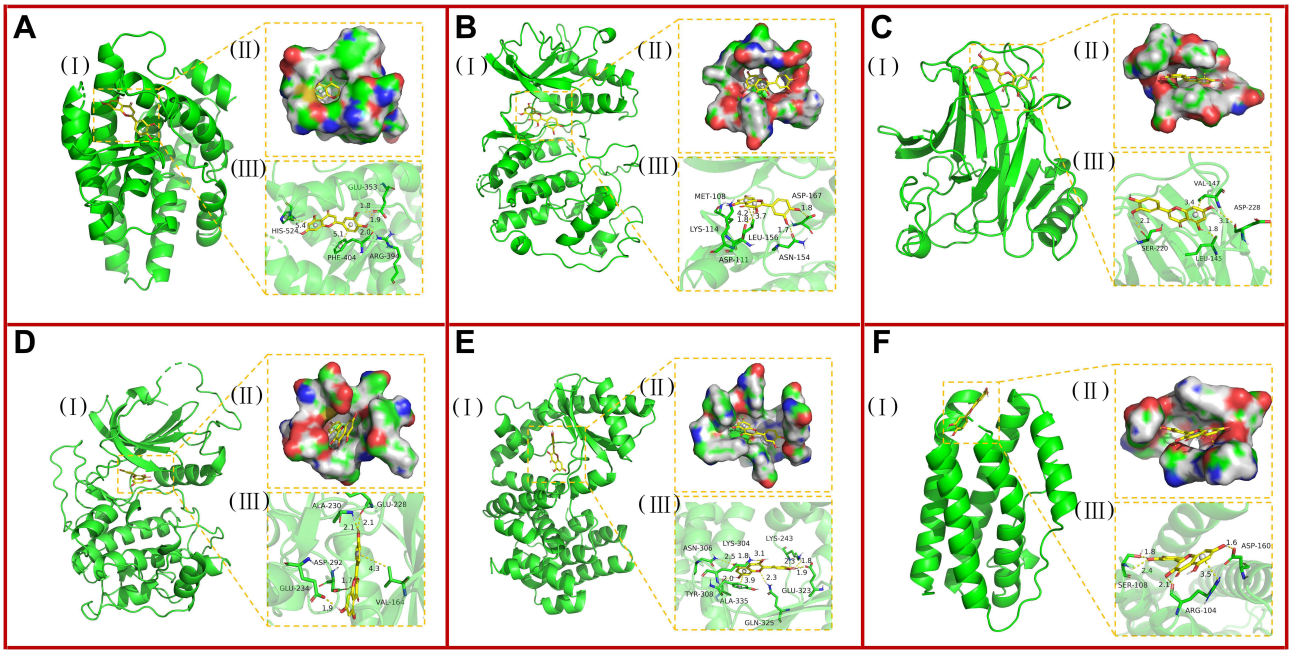

Figure 5 The binding mode of protein with compound. (**A**) The binding mode of ESR1 protein with Luteolin. (**B**) The binding mode of MAPK1 protein with Quercetin. (**C**) The binding mode of TP53 protein with Luteolin. (**D**) The binding mode of AKT1 protein with Kaempferol. (**E**) The binding mode of RELA protein with Quercetin. (**F**) The binding mode of IL6 protein with Quercetin. Each picture shows three areas: (I) The 3D structure of complex. (II) The surface of active site. (III) The detail binding mode of complex. The backbone of protein is rendered in tube and colored in green. Compound is rendering by yellow. Yellow dash represents hydrogen bond distance or π-stacking.

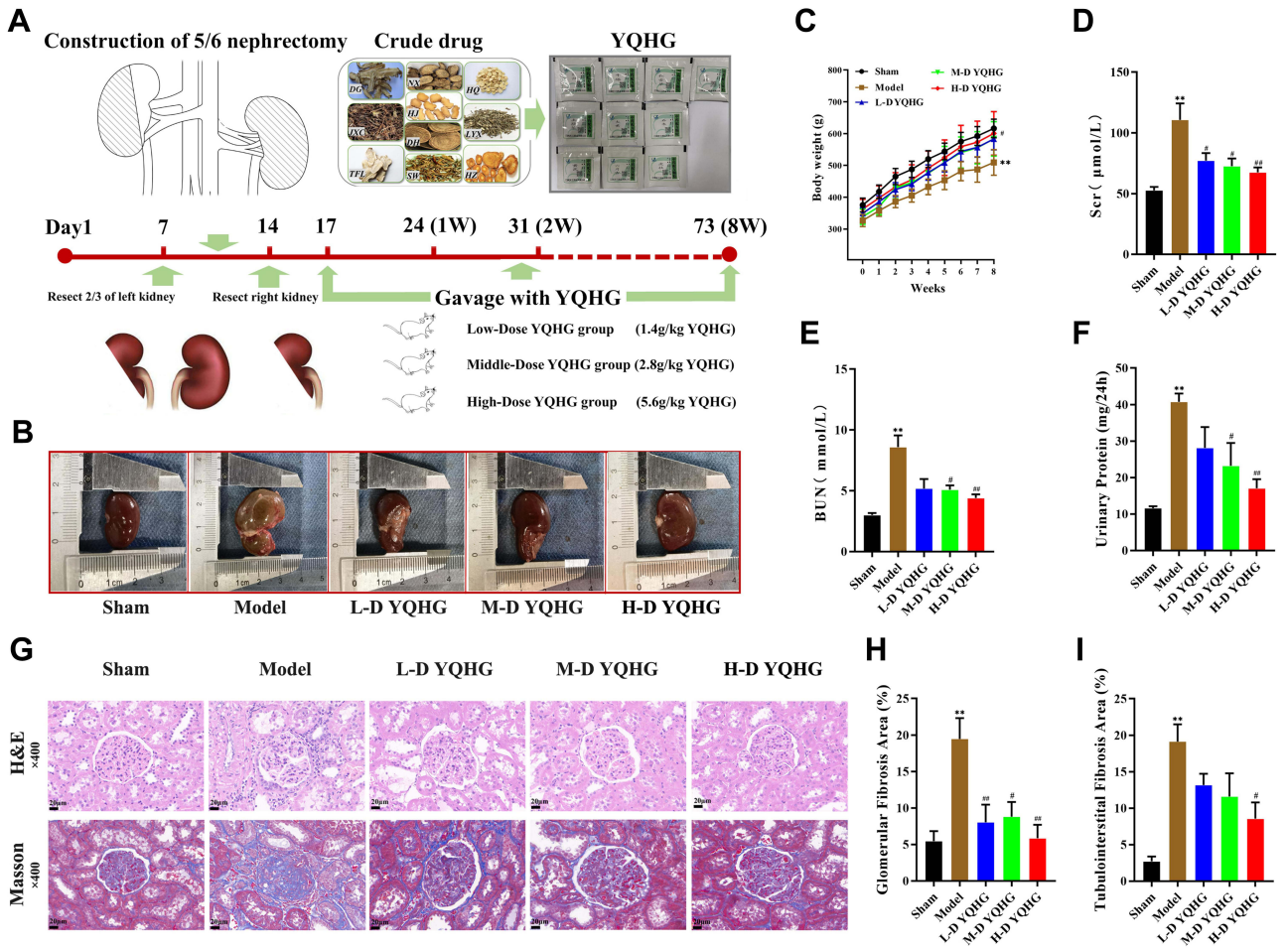

Figure 6 YQHG improves kidney function and fibrosis in 5/6 nephrectomized rats. (**A**) Construction of 5/6 nephrectomy model and YQHG dosing schedule. (**B**) The kidney of the rats was photographed (n=6). (**C**) The body weight of the rats was measured (n=6). (**D–F**) Effects of YQHG treatment on levels of Scr, BUN, and urinary protein in 5/6 nephrectomized rats (n=6). (**G**) Representative images of H&E (40×Magnification, Scale bar 20μm) staining and Masson (40×Magnification, scale bar 20μm) staining of kidney tissues (n=6). (**H–I**) Quantitative analysis of glomerular fibrosis area and tubulointerstital fibrosis area based on Masson staining (n=6). All data are expressed as mean±SEM. For normally distributed data (body weight, Scr, urinary protein, glomerular fibrosis area, tubulointerstital fibrosis area), one-way ANOVA followed by Tukey's test was used. For non-normally distributed data (BUN), Kruskal–Wallis test followed by non-parametric Wilcoxon rank-sum test was used. $^{**}P < 0.01$ vs the sham group; $^{\#}P < 0.05$, $^{\#\#}P < 0.01$ vs the model group.

Discussion

Yishen Qingli Heluo granule (YQHG) is representative traditional Chinese medicine (TCM) remedy for clinical treatment of CKD.[35] Network pharmacology is considered as novel and effective method to clarify the underlying mechanisms of complex TCM herbs, which is consistent with the holistic view of TCM. Therefore, based on various available databases and software, we applied network pharmacology to explore the potential mechanisms of YQHG in the treatment of CKD. At the same time, animal experiments were conducted to verify the reliability of the network pharmacology results. In this study, a CKD rat model was constructed by 5/6 nephrectomy. Removal of 5/6 kidney parenchyma effectively reduces the number of nephrons, which in turn leads to elevated perfusion, filtration and pressure in the residual nephrons. Persistent overload leads to 1/6 remnant kidney unable to maintain homeostasis, which ultimately contributes to the gradual loss of renal function.[36] At present, the 5/6 nephrectomy model has been recognized as the classical model most similar to human CKD. It completely simulates the disease process from acute renal failure to renal function compensation and decompensation. The model rats with 10-week duration 5/6 nephrectomy tended to belong to the stage of decompensation. It has been widely used to study the therapeutic effect of drugs on CKD.[37–39] Moreover, the 5/6 nephrectomy model also show significant gut microbiota dysbiosis,[40,41] and this model may be suitable in this study.

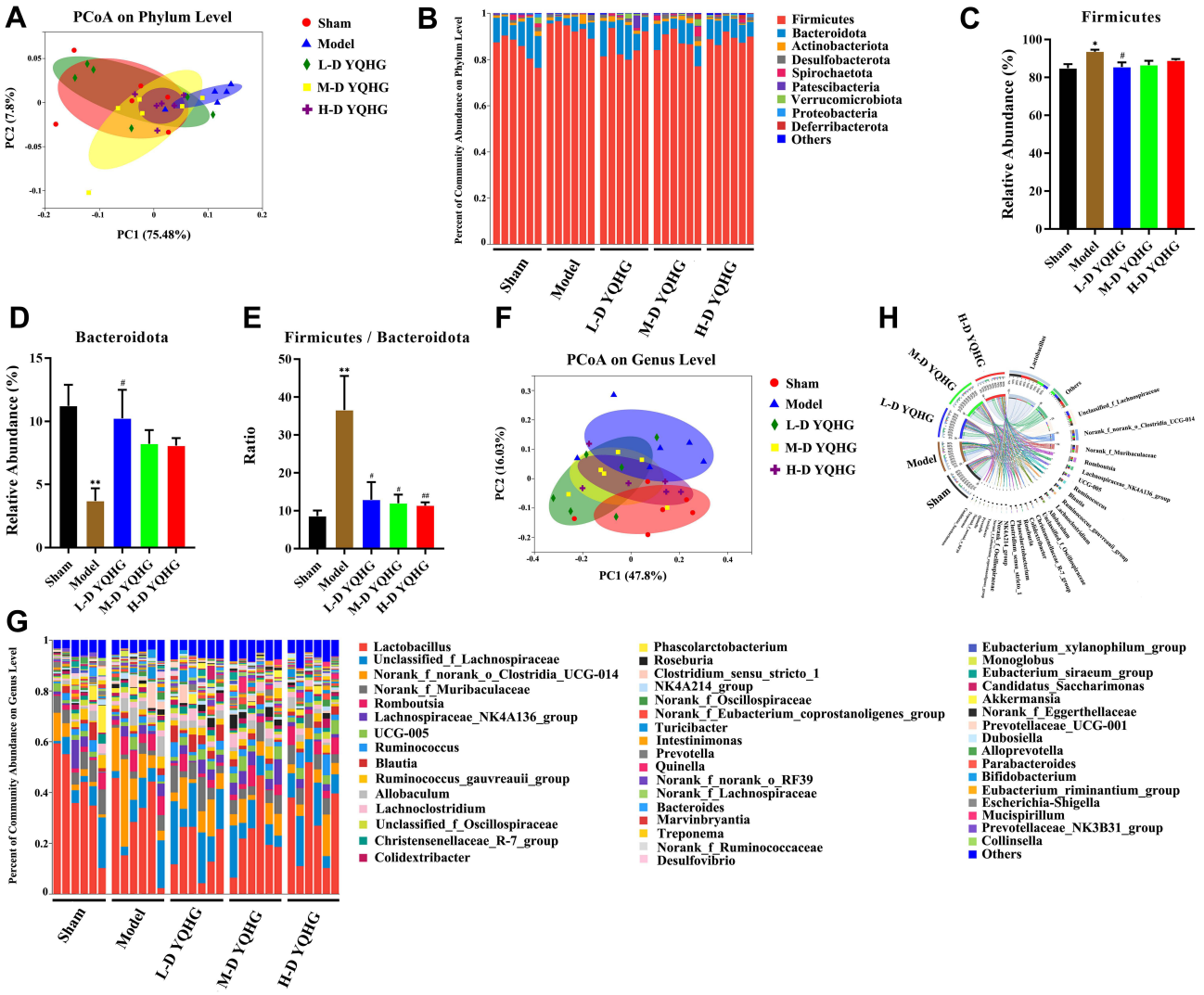

Figure 7 YQHG reshaped gut microbiota by reducing Firmicutes/Bacteroidota ratio in 5/6 nephrectomized rats. (**A**) PCoA on phylum level (n=6). (**B**) Relative abundance of gut microbiota on phylum level (n=6). (**C** and **D**) Relative abundance of Firmicutes and Bacteroidota on phylum level (n=6). (**E**) The ratio of Firmicutes/Bacteroidota on phylum level (n=6). (**F**) PCoA on genus level (n=6). (**G**) Relative abundance of gut microbiota on genus level (n=6). (**H**) Circos diagram of species-sample relationship on genus level (n=6). The small semicircle (left half circle) indicates the composition of the gut microbiota in each group, the color of the outer ribbon represents which group it comes from, the color of the inner ribbon represents the gut microbiota, and the length represents the relative abundance of gut microbiota in the corresponding group; the large semicircle (right half circle) indicates the distribution ratio of gut microbiota in different groups on genus level. The outer color band represents the gut microbiota, the inner color band represents different groups, and the length represents the distribution ratio of the group in a certain gut microbiota. All data are expressed as mean±SEM. For normally distributed data (Firmicutes, Bacteroidota), one-way ANOVA followed by Tukey's test was used. For non-normally distributed data (Firmicutes/Bacteroidota), Kruskal–Wallis test followed by non-parametric Wilcoxon rank-sum test was used. $^{*}P < 0.05$, $^{**}P < 0.01$ vs the sham group; $^{\#}P < 0.05$, $^{\#\#}P < 0.01$ vs the model group.

Our present study clearly indicated that YQHG treatment significantly prevented the progression of CKD, characterized by increased body weight, improved kidney appearance and function, reduced tissue damage in 5/6 nephrectomized rats. Regardless of the cause, kidney fibrosis is a common result of most progressive kidney diseases and is closely related to worsening kidney function. Importantly, we demonstrated that 5/6 nephrectomized rats treated with YQHG showed a significant improvement in kidney fibrosis, as evidenced by the reduction in the area of glomerular and tubulointerstitial fibrosis. Therefore, our results suggested that YQHG had a comprehensive protective effect on kidney function and fibrosis.

More importantly, based on H-CT network, we discovered that the 10 herbs in YQHG shared a common target, which was PTGS2. The existence of this target was a manifestation of the synergistic effect of TCM, which may be involved in the pathological process of CKD. PTGS2 is pro-inflammatory enzyme, which is major pharmaceutical targets for anti-inflammatory medicine.[42] Adesso et al found that PTGS2 was involved in the regulation of inflammatory processes in

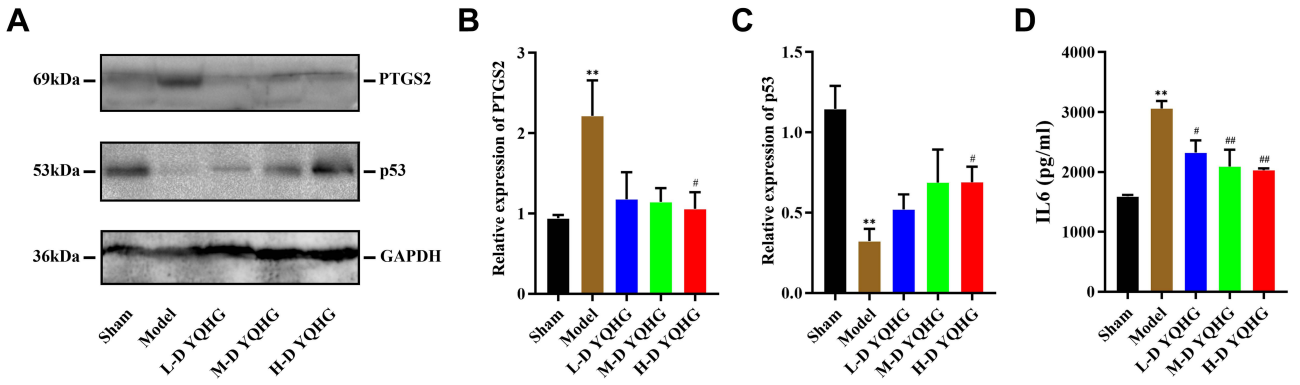

Figure 8 YQHG regulates the expression of PTGS2, p53 and IL-6 in 5/6 nephrectomized rats. (**A**) Representative Western blots for PTGS2, p53 and GAPDH protein expression in kidney tissue (n=6). (**B**) Relative expression of PTGS2 (n=6). (**C**) Relative expression of p53 (n=6). (**D**) Expression of IL6 in kidney tissue was determined by ELISA. All data are expressed as mean±SEM. For non-normally distributed data (PTGS2, p53, IL6), Kruskal–Wallis test followed by non-parametric Wilcoxon rank-sum test was used. $^{**}P < 0.01$ vs the sham group; $^{\#}P < 0.05$, $^{\#\#}P < 0.01$ vs the model group.

CKD.[43] The activation of the inflammatory cascade leads to the accumulation of inflammatory factors in the target organs, thereby inducing tissue fibrosis to a certain extent, and ultimately promoting the development of diseases. Therefore, some studies focused on exploring the relationship between PTGS2 and fibrosis of certain target organs,[44–46] including the kidney.[47,48] These results suggested that reduced expression of PTGS2 may contribute to the alleviation of tissue inflammation and fibrosis. In support of this notion, our data revealed that H-D YQHG treatment significantly decreased the expression of PTGS2 in kidney tissue. Moreover, the area of glomerular and tubulointerstital fibrosis was marked decreased in our study, which had been mentioned above.

KEGG enrichment analysis showed that p53 was a key signaling pathway involved in YQHG against CKD. P53, a well-known tumor suppressor, has been found to play a role in AKI and subsequent kidney repair by regulating cell apoptosis and autophagy.[49] Our study found that H-D YQHG could up-regulate the expression of p53 to a certain extent. In addition, GO biological process enrichment analysis also revealed the potential role of YQHG in regulating cell apoptosis. These results suggested that the mechanism of YQHG on CKD may involve the regulation of cell apoptosis. In follow-up mechanistic studies, we need further proof (eg, TUNEL assay, transcript level analysis) for the above findings.

In the present study, a C-T network of YQHG was constructed using the 63 active compounds and 250 responding targets. The results indicated that Quercetin, Kaempferol, Luteolin, 7-O-methylisomucronulatol, Wogonin, and Stigmasterol were the top 6 active compounds in YQHG. Therefore, they may be the key pleiotropic active compounds of YQHG and exert their potential biological effects in the treatment of CKD through multiple targets. These six crucial compounds are representative flavonoids, which have protective effects on CKD-related pathological processes. To further verify the accuracy of network pharmacology, the binding affinity between the six active compounds and hub proteins (TP53, AKT1, RELA, IL6, MAPK1, ESR1) was analyzed by molecular docking method. The results indicated that compounds with the best binding mode to the six targets were Quercetin, Kaempferol, Luteolin. Quercetin has been shown to exert multiple pharmacological activities, such as anti-inflammatory, anti-oxidant, anti-fibrosis, anti-thrombotic, anti-tumor and vasodilation effects.[50] Among these pharmacological activities, the potential of Quercetin to reduce the occurrence and development of CKD by alleviating tubulointerstital fibrosis has also been continuously reported. It is reported that Quercetin was able to alleviate TGF-β-induced fibrosis in kidney tubular epithelial cells by suppressing miR-21.[51] Notably, Quercetin is currently in a clinical trial for treating diabetic nephropathy. The above studies provide an important basis for further clinical research of YQHG on CKD.[52] Kaempferol significantly reduced kidney inflammation, fibrosis and dysfunction in mice with streptozotocin-induced diabetic nephropathy.[53] Luteolin was reported to ameliorate glomerular sclerosis and interstitial fibrosis in mice with diabetic nephropathy.[54] More importantly our results suggested that IL6 may serve as a potential target of YQHG against CKD. First, our data showed that the binding affinity of Quercetin to IL6 was less than −5 kcal/mol, indicating that they possessed good binding activity. In addition, previous studies reported that the reduction of IL6 expression may contribute to alleviate tissue inflammation and fibrosis in CKD

rats.[55,56] Our current study found that YQHG treatment decreased the expression of IL6 in kidney tissue, which was consistent with previous results. The above results provided a good clue that IL6 may become a potential target of YQHG against CKD.

The efficacy of TCM herbal treatment is closely related to its influence on the profile of gut microbiota. The active compounds of TCM herbs may not only directly regulate host cell activity, but is also metabolized by gut microbiota.[57,58] Therefore, the disordered gut microbiota may affect the efficacy of TCM herbs in treating diseases. Notably, the gut microbiota of rats treated with YQHG was reshaped in our study, which was characterized by a decrease in the ratio of F/B. The reduced F/B ratio was often considered to be an indicator for the restoration of gut microbiota balance, which had been reported in previous studies.[56,59,60] Therefore, the results suggested that the protective effect of YQHG may be partly attributed to the mediation of the gut microbiota. Based on the microbiota-transfer study (co-housing and fecal microbiota transplantation), future studies need to verify how the gut microbiota mediates the therapeutic effect of YQHG on CKD and to explore its impact on these key active compounds and targets.

Limitations

(1) However, CKD can result from multiple causes (for instance diabetic nephropathy is not the same as autoimmune disease-related CKD etc.) and therefore the key active compounds and targets of YQHG will need to be tested in additional models. (2) Moreover, current animal/cell models could not replicate all the features of human CKD. Staining these markers in human samples or detecting their expression levels in CKD patients will be the focus of follow-up studies. (3) The liver function, blood count and other related parameters of the treated rats can be tested to comprehensively evaluate the safety of the drug. The six active compounds of YQHG for the treatment of CKD were based on network pharmacology and molecular docking, and more extensive experiments (eg, plasma concentration determination of the six active compounds) will be required to provide more evidence in the future.

Conclusion

In summary, we explored the potential mechanism of YQHG against CKD based on network pharmacology and experimental validation. Our preliminarily conclusion is that YQHG can be used for treating CKD by regulating the p53 signaling pathway, and inhibiting the expression of PTGS2, IL6. Notably, the homeostasis of gut microbiota was closely related to the therapeutic effects of TCM on diseases. The present results showed that YQHG was a potential regulator of gut microbiota by reducing the F/B ratio. Our current finding suggests that YQHG may become a novel promising TCM granule for the treatment of CKD. It would be interesting if YQHG is also effective for acute injury, which is worth exploring further. At the same time, we propose that the "Compound-Target-Gut microbiota" databases based on TCM herbs can be constructed in the future.

Abbreviations

CKD, chronic kidney disease; TCM, traditional chinese medicine; OB, oral bioavailability; DL, drug-likeness; GO, gene ontology; KEGG, Kyoto Encyclopedia of Genes and Genomes; SD, Sprague Dawley; Scr, serum creatinine; BUN, blood urea nitrogen.

Funding

This research was funded by National Natural Science Foundation of the People's Republic of China (grant number 82174295) and Graduate Research and Practice Innovation Program of Jiangsu Province Graduate Student Cultivation Innovative Engineering (grant number SJCX21_0781).

Disclosure

All authors declare no conflicts of interest.

References

1. Bikbov B, Purcell CA, Levey AS; GBD Chronic Kidney Disease Collaboration. Global, regional, and national burden of chronic kidney disease, 1990–2017: a systematic analysis for the Global Burden of Disease Study 2017. *Lancet*. 2020;395(10225):709–733. doi:10.1016/S0140-6736(20)30045-3
2. Chung EY, Ruospo M, Natale P, et al. Aldosterone antagonists in addition to renin angiotensin system antagonists for preventing the progression of chronic kidney disease. *Cochrane Database Syst Rev*. 2020;10(10):CD007004. doi:10.1002/14651858.CD007004
3. Hsu TW, Liu JS, Hung SC, et al. Renoprotective effect of renin-angiotensin-aldosterone system blockade in patients with predialysis advanced chronic kidney disease, hypertension, and anemia. *JAMA Intern Med*. 2014;174(3):347–354. doi:10.1001/jamainternmed.2013.12700
4. Zeeuw DD. Unmet need in renal protection–do we need a more comprehensive approach? *Contrib Nephrol*. 2011;171:157–160. doi:10.1159/000327337
5. Chan YH, Ma LT, Tullus K. When should we start and stop ACEi/ARB in paediatric chronic kidney disease? *Pediatr Nephrol*. 2021;36(7):1751–1764. doi:10.1007/s00467-020-04788-w
6. Zhang Y, He D, Wei Z, et al. ACE inhibitor benefit to kidney and cardiovascular outcomes for patients with non-dialysis chronic kidney disease stages 3–5: a network meta-analysis of randomised clinical trials. *Drugs*. 2020;80(8):797–811. doi:10.1007/s40265-020-01290-3
7. Sipahi I, Debanne SM, Rowland DY, Simon DI, Fang JC. Angiotensin-receptor blockade and risk of cancer: meta-analysis of randomised controlled trials. *Lancet Oncol*. 2010;11(7):627–636. doi:10.1016/S1470-2045(10)70106-6
8. Bangalore S, Sunil K, Kjeldsen SE, et al. Antihypertensive drugs and risk of cancer: network meta-analyses and trial sequential analyses of 324,168 participants from randomised trials. *Lancet Oncol*. 2011;12(1):65–82. doi:10.1016/S1470-2045(10)70260-6
9. Liyanage T, Ninomiya T, Jha V, et al. Worldwide access to treatment for end-stage kidney disease: a systematic review. *Lancet*. 2015;385(9981):1975–1982. doi:10.1016/S0140-6736(14)61601-9
10. Liu SY, Huang P, Zhang N. Efficacy and safety of the Fu-Zheng-Qu-Zhuo method on retarding the progress of chronic kidney disease (stage 3–4): a systematic review and meta-analysis. *Ann Transl Med*. 2019;7(6):114. doi:10.21037/atm.2018.12.29
11. Zheng L, Chen S, Wang F, et al. Distinct responses of gut microbiota to Jian-Pi-Yi-Shen Decoction are associated with improved clinical outcomes in 5/6 nephrectomized rats. *Front Pharmacol*. 2020;11:604. doi:10.3389/fphar.2020.00604
12. Zhou SS, Ai ZZ, Li WN, et al. Deciphering the pharmacological mechanisms of Taohe-Chengqi Decoction extract against renal fibrosis through integrating network pharmacology and experimental validation in vitro and in vivo. *Front Pharmacol*. 2020;11:425. doi:10.3389/fphar.2020.00425
13. Chen JH, Sheng MX, Xu LD, et al. Evaluation of clinical efficacy of Yishen Qingli Xiezhuo Decoction on patients with CKD stage 3 based on real world principles. *Modern Trad Chin Med Materia Medica-World Sci Technol*. 2019;21(6):1055–1061. doi:10.11842/wst.2019.06.003
14. Zhao J, Chen JH, Hou Y, Sun W, Jiang M. Clinical effect of Yishen Qingli Heluo granule on urinary protein, serum creatinine and eGFR in patients with CKD3 patients. *J Chin Med Mater*. 2017;40(11):2701–2705. doi:10.13863/j.issn1001-4454.2017.11.046
15. Liu H, Gu LB, Tu Y, Hu H, Huang YR, Wei S. Emodin ameliorates cisplatin-induced apoptosis of rat renal tubular cells in vitro by activating autophagy. *Acta Pharmacol Sin*. 2016;37(2):235–245. doi:10.1038/aps.2015.114
16. Zheng JH, Wu M, Wang HY, et al. Network pharmacology to unveil the biological basis of health-strengthening herbal medicine in cancer treatment. *Cancers*. 2018;10(11):461. doi:10.3390/cancers10110461
17. Tao B, Wang Q, Cao JG, et al. The mechanisms of Chuanxiong Rhizoma in treating spinal cord injury based on network pharmacology and experimental verification. *Ann Transl Med*. 2021;9(14):1145. doi:10.21037/atm-21-2529
18. Feng SH, Zhao B, Zhan X, Motanyane R, Wang SM, Li A. Danggui Buxue Decoction in the treatment of metastatic colon cancer: network pharmacology analysis and experimental validation. *Drug Des Devel Ther*. 2021;15:705–720. doi:10.2147/DDDT.S293046
19. Gu LF, Hong F, Fan KK, et al. Integrated network pharmacology analysis and pharmacological evaluation to explore the active components and mechanism of Abelmoschus manihot (L.) Medik. on renal fibrosis. *Drug Des Devel Ther*. 2020;14:4053–4067. doi:10.2147/DDDT.S264898
20. Fang J, Sun XQ, Xue BY, Fang NY, Zhou M. Dahuang Zexie Decoction protects against high-fat diet-induced NAFLD by modulating gut microbiota-mediated toll-like receptor 4 signaling activation and loss of intestinal barrier. *Evid Based Complement Alternat Med*. 2017;2017:2945803. doi:10.1155/2017/2945803
21. Chen MT, Xie Y, Gong SL, et al. Traditional Chinese medicine in the treatment of nonalcoholic steatohepatitis. *Pharmacol Res*. 2021;172:105849. doi:10.1016/j.phrs.2021.105849
22. Li QM, Cui Y, Xu BC, et al. Main active components of Jiawei Gegen Qinlian decoction protects against ulcerative colitis under different dietary environments in a gut microbiota-dependent manner. *Pharmacol Res*. 2021;170:105694. doi:10.1016/j.phrs.2021.105694
23. Xu J, Chen HB, Li SL. Understanding the molecular mechanisms of the interplay between herbal medicines and gut microbiota. *Med Res Rev*. 2017;37(5):1140–1185. doi:10.1002/med.21431
24. Ru JL, Li P, Wang JN, et al. TCMSP: a database of systems pharmacology for drug discovery from herbal medicines. *J Cheminform*. 2014;6:13. doi:10.1186/1758-2946-6-13
25. Szklarczyk D, Gable AL, Lyon D, et al. STRING v11: protein-protein association networks with increased coverage, supporting functional discovery in genome-wide experimental datasets. *Nucleic Acids Res*. 2019;47(D1):607–613. doi:10.1093/nar/gky1131
26. Yu GC, Wang LG, Han YY, He QY. clusterProfiler: an R package for comparing biological themes among gene clusters. *OMICS*. 2012;16(5):284–287. doi:10.1089/omi.2011.0118
27. Gaillard T. Evaluation of AutoDock and AutoDock Vina on the CASF-2013 Benchmark. *J Chem Inf Model*. 2018;58(8):1697–1706. doi:10.1021/acs.jcim.8b00312
28. Sharkey I, Boddy AV, Wallace H, Mycroft J, Hollis R, Picton S. Body surface area estimation in children using weight alone: application in paediatric oncology. *Br J Cancer*. 2001;85(1):23–28. doi:10.1054/bjoc.2001.1859
29. Yu YH, Kim SW, Park DK, et al. Altered emotional phenotypes in chronic kidney disease following 5/6 nephrectomy. *Brain Sci*. 2021;11(7):882. doi:10.3390/brainsci11070882
30. Peng Y, Zhang SY, Liu ZW, et al. Gut microbiota and Chinese medicine syndrome: altered fecal microbiotas in spleen (Pi)-deficient patients. *J Tradit Chin Med*. 2020;40(1):137–143. PMID: 32227775.
31. Lin TL, Lu CC, Lai WF, et al. Role of gut microbiota in identification of novel TCM-derived active metabolites. *Protein Cell*. 2021;12(5):394–410. doi:10.1007/s13238-020-00784-w

32. Bi TT, Feng RQ, Zhan LB, Ren WM, Lu XG. ZiBuPiYin recipe prevented and treated cognitive decline in ZDF rats With diabetes-associated cognitive decline via microbiota-gut-brain axis dialogue. *Front Cell Dev Biol*. 2021;9:651517. doi:10.3389/fcell.2021.651517
33. Xu XZ, Gao ZZ, Yang FQ, et al. Antidiabetic effects of Gegen Qinlian Decoction via the gut microbiota are attributable to its key ingredient Berberine. *Genomics Proteomics Bioinformatics*. 2020;18(6):721–736. doi:10.1016/j.gpb.2019.09.007
34. Lv J, Jia YT, Li J, et al. Gegen Qinlian decoction enhances the effect of PD-1 blockade in colorectal cancer with microsatellite stability by remodelling the gut microbiota and the tumour microenvironment. *Cell Death Dis*. 2019;10(6):415. doi:10.1038/s41419-019-1638-6
35. Zhao J, He W, Gao K, et al. Theoretical origin of the core pathogenesis of "Kidney Deficiency, Dampness and Stasis" of Chronic Kidney Disease. *Modern Trad Chin Med Materia Medica-World Sci Technol*. 2019;21(6):1085–1088. doi:10.11842/wst.2019.06.007
36. Kujal P, Vernerová Z. 5/6 nephrectomy as an experimental model of chronic renal failure and adaptation to reduced nephron number. *Cesk Fysiol*. 2008;57(4):104–109. PMID: 19526664.
37. López-Baltanás R, Rodríguez-Ortiz ME, Antonio C, et al. Magnesium supplementation reduces inflammation in rats with induced chronic kidney disease. *Eur J Clin Invest*. 2021;51(8):e13561. doi:10.1111/eci.13561
38. Zhou FY, Zou XH, Zhang J, Wang ZW, Yang YJ, Wang DT. Jian-Pi-Yi-Shen formula ameliorates oxidative stress, inflammation, and apoptosis by activating the Nrf2 signaling in 5/6 nephrectomized rats. *Front Pharmacol*. 2021;12:630210. doi:10.3389/fphar.2021.630210
39. Mizukami K, Yoshida H, Nozawa E, Wada K, Ugawa T. Renoprotective effects of the novel prostaglandin EP4 receptor-selective antagonist ASP7657 in 5/6 nephrectomized chronic kidney disease rats. *Naunyn Schmiedebergs Arch Pharmacol*. 2019;392(4):451–459. doi:10.1007/s00210-018-01600-3
40. Liu Y, Li JP, Yu JG, et al. Disorder of gut amino acids metabolism during CKD progression is related with gut microbiota dysbiosis and metagenome change. *J Pharm Biomed Anal*. 2018;149:425–435. doi:10.1016/j.jpba.2017.11.040
41. Feng YL, Cao G, Chen DQ, et al. Microbiome-metabolomics reveals gut microbiota associated with glycine-conjugated metabolites and polyamine metabolism in chronic kidney disease. *Cell Mol Life Sci*. 2019;76(24):4961–4978. doi:10.1007/s00018-019-03155-9
42. Basudhar D, Glynn SA, Greer M, et al. Coexpression of NOS2 and COX2 accelerates tumor growth and reduces survival in estrogen receptor-negative breast cancer. *Proc Natl Acad Sci U S A*. 2017;114(49):13030–13035. doi:10.1073/pnas.1709119114
43. Adesso S, Popolo A, Bianco G, et al. The uremic toxin indoxyl sulphate enhances macrophage response to LPS. *PLoS One*. 2013;8(9):e76778. doi:10.1371/journal.pone.0076778
44. Wang YD, Wei YH, He N, et al. Evaluation of cyclooxygenase-2 fluctuation via a near-infrared fluorescent probe in idiopathic pulmonary fibrosis cell and mice models. *J Mater Chem B*. 2021;9(31):6226–6233. doi:10.1039/d1tb01307f
45. Feng S, Tong H, Gao JH, et al. Anti-inflammation treatment for protection of hepatocytes and amelioration of hepatic fibrosis in rats. *Exp Ther Med*. 2021;22(5):1213. doi:10.3892/etm.2021.10647
46. Zhang LH, Tai Y, Zhao C, et al. Inhibition of cyclooxygenase-2 enhanced intestinal epithelial homeostasis via suppressing β-catenin signalling pathway in experimental liver fibrosis. *J Cell Mol Med*. 2021;25(16):7993–8005. doi:10.1111/jcmm.16730
47. Chang JF, Yeh JC, Ho CT, et al. Targeting ROS and cPLA2/COX2 Expressions ameliorated renal damage in obese mice with endotoxemia. *Int J Mol Sci*. 2019;20(18):4393. doi:10.3390/ijms20184393
48. Nelson T, Velazquez H, Troiano N, Fretz JA. Early B Cell Factor 1 (EBF1) Regulates glomerular development by controlling mesangial maturation and consequently COX-2 expression. *J Am Soc Nephrol*. 2019;30(9):1559–1572. doi:10.1681/ASN.2018070699
49. Tang CY, Ma ZW, Zhu JF, et al. P53 in kidney injury and repair: mechanism and therapeutic potentials. *Pharmacol Ther*. 2019;195:5–12. doi:10.1016/j.pharmthera.2018.10.013
50. Ebrahimpour S, Zakeri M, Esmaeili A. Crosstalk between obesity, diabetes, and Alzheimer's disease: introducing Quercetin as an effective triple herbal medicine. *Ageing Res Rev*. 2020;62:101095. doi:10.1016/j.arr.2020.101095
51. Cao YC, Hu JL, Sui JY, Jiang LM, Cong YK, Ren GQ. Quercetin is able to alleviate TGF-β-induced fibrosis in renal tubular epithelial cells by suppressing miR-21. *Exp Ther Med*. 2018;16(3):2442–2448. doi:10.3892/etm.2018.6489
52. Hickson LJ, Langhi Prata LGP, Bobart SA, et al. Senolytics decrease senescent cells in humans: preliminary report from a clinical trial of Dasatinib plus Quercetin in individuals with diabetic kidney disease. *EBioMedicine*. 2019;47:446–456. doi:10.1016/j.ebiom.2019.08.069
53. Luo W, Chen XJ, Ye L, et al. Kaempferol attenuates streptozotocin-induced diabetic nephropathy by downregulating TRAF6 expression: the role of TRAF6 in diabetic nephropathy. *J Ethnopharmacol*. 2021;268:113553. doi:10.1016/j.jep.2020.113553
54. Zhang MY, He LY, Liu JS, Zhou L. Luteolin attenuates diabetic nephropathy through suppressing inflammatory response and oxidative stress by inhibiting STAT3 pathway. *Exp Clin Endocrinol Diabetes*. 2021;129(10):729–739. doi:10.1055/a-0998-7985
55. Bian XH, Bai Y, Su XX, Zhao GF, Sun GP, Li D. Knockdown of periostin attenuates 5/6 nephrectomy-induced intrarenal renin-angiotensin system activation, fibrosis, and inflammation in rats. *J Cell Physiol*. 2019;234(12):22857–22873. doi:10.1002/jcp.28849
56. Santos-Marcos JA, Perez-Jimenez F, Camargo A. The role of diet and intestinal microbiota in the development of metabolic syndrome. *J Nutr Biochem*. 2019;70:1–27. doi:10.1016/j.jnutbio.2019.03.017
57. Dey P. Gut microbiota in phytopharmacology: a comprehensive overview of concepts, reciprocal interactions, biotransformations and mode of actions. *Pharmacol Res*. 2019;147:104367. doi:10.1016/j.phrs.2019.104367
58. Lin TL, Shu CC, Lai WF, Tzeng CM, Lu CC. Investiture of next generation probiotics on amelioration of diseases-Strains do matter. *Med Microecol*. 2019;1–2(2019):100002. doi:10.1016/j.medmic.2019.100002
59. Cattò C, Garuglieri E, Borruso L, et al. Impacts of dietary silver nanoparticles and probiotic administration on the microbiota of an in-vitro gut model. *Environ Pollut*. 2019;245:754–763. doi:10.1016/j.envpol.2018.11.019
60. McCabe LR, Irwin R, Tekalur A, et al. Exercise prevents high fat diet-induced bone loss, marrow adiposity and dysbiosis in male mice. *Bone*. 2019;118:20–31. doi:10.1016/j.bone.2018.03.024